*1997 HST Calibration Workshop*
*Space Telescope Science Institute, 1997*
*S. Casertano, et al., eds.*

# The Photometric Performance of NICMOS

L. Colina[1]

*Space Telescope Science Institute, 3700 San Martin Drive, MD 21218*

M.J. Rieke

*University of Arizona, Steward Observatory, Tucson, AZ 85721*

**Abstract.** This contribution reviews our current understanding of NICMOS photometric characteristics paying special attention to the absolute calibration of NICMOS detectors and the sources of systematic uncertainty when performing the calibration. Preliminary results based on SMOV and Cycle 7 calibration programs are presented.

## 1. Introduction

The near-infrared wavelength range was opened to HST with the installation of the Near-Infrared Camera and Multi-Object Spectrometer (NICMOS) last February, during the second HST servicing mission. Unaffected by atmospheric absorption and emission, NICMOS covers the entire 0.8 $\mu$m to 2.5 $\mu$m wavelength range. Similarly, NICMOS, being above the atmosphere, is not forced to adopt filter bandpasses like those used at ground-based observatories matching the near-infrared atmospheric windows. In practice NICMOS does not have a set of filters matching any of the standard ground-based photometric bands and this poses a challenge when trying to achieve precise absolute photometry. On the other hand, NICMOS absolute calibration requires a set of faint spectrophotometric standards covering the entire 0.8–2.5$\mu$m wavelength range. Such a set of standards didn't exist before and the selection and generation of NICMOS standards represented additional challenges.

This paper reviews the several steps taken to ensure accurate absolute calibration of the NICMOS detectors. Details on NICMOS absolute spectrophotometric standards are given in Section 2. Section 3 discusses some of the sources of uncertainties when performing absolute calibration with NICMOS. The results of the first on-orbit absolute calibration of NICMOS are given in Section 4 while Section 5 mentions the transformation of the HST photometric system into JHK ground-based systems. Section 6 describes future plans towards the characterization of NIC3 photometric performance. This paper does not mention the performance of the NIC3 GRISMs as they will be the topic of a separate contribution (Freudling 1997).

## 2. Absolute Spectrophotometric Standards for NICMOS

The absolute calibration of the ultraviolet and optical instruments onboard HST is based on the existence of absolutely calibrated spectra of a few pure hydrogen white dwarfs (WD) and hot stars, the so-called HST set of absolute spectrophotometric standards (Colina & Bohlin 1994; Bohlin, Colina & Finley 1995; Bohlin 1996). The absolute calibration of the set of HST absolute standards in the UV and optical, is based on a detailed model of

[1]Affiliated with the Astrophysics Division, Space Science Department, ESA

the primary standard G191-B2B, a hot pure hydrogen white dwarf, after normalization to accurate Landolt visual photometry (Bohlin et al., 1995; Bohlin 1996). This model covers the entire NICMOS wavelength range and therefore G191-B2B has been selected as the primary NICMOS WD standard.

An alternative method for calibrating NICMOS uses solar analogs (Campins et al., 1985). Three faint solar analogs were selected by the NICMOS Investigation Definition Team (IDT), and observed repeatedly on the ground at JHK (E. Green and E. Persson, private communication). Spectra of these three solar analogs were taken with the HST Faint Object Spectrograph (FOS) in the 0.2–0.8$\mu$m wavelength range to study how accurately their spectral energy distribution matched that of the Sun (Colina & Bohlin 1997). The absolute flux distribution of these three solar analogs covering the ultraviolet to near-infrared range was obtained by combining a scaled version of an absolutely calibrated solar reference spectrum (Colina, Bohlin & Castelli 1996) with the FOS spectra (Colina & Bohlin 1997). In the near-infrared, the solar reference spectrum was generated by computing the energy output of a solar photospheric model using the most recent version of Kurucz ATLAS code (see Colina et al., 1996 for details). Of the three solar analogs, P330E was selected as the primary NICMOS solar analog standard.

## 3. NICMOS Absolute Photometry: Sources of Uncertainty

### 3.1. Absolute Spectrophotometric Standards

One white dwarf (G191-B2B) and one solar analog (P330E) have been selected as NICMOS primary spectrophotometric standards. To assess the accuracy of the G191-B2B model in the near-infrared, two state-of-the-art atmosphere flux distributions for exactly the same physical parameters were computed independently by two different experts in this field. The largest differences in the continuum fluxes of the two independent models were 3.5% in the near-infrared at 2.5$\mu$m (Bohlin 1996).

The spectral energy distribution of P330E in the 0.4–0.8$\mu$m range is the same as the solar reference spectrum, within the uncertainties of the FOS measurements (Colina & Bohlin 1997). The near-infrared spectrum of P330E, created by rescaling the reference spectrum of the Sun (see Colina & Bohlin 1997 for details), agrees to within 2–3% with ground-based near-infrared photometry.

In summary, the accuracy of the absolute spectral energy distribution of NICMOS primary standards introduces a systematic uncertainty of about 2–3% in the absolute calibration of the different filters.

### 3.2. Differential Photometry Accross Detectors

The photometric values provided in the headers are obtained from measurements of standard stars in the central regions of the detectors. Both high frequency (i.e. pixel-to-pixel) and low frequency (i.e. large scale structures) sensitivity variations will be corrected using on-orbit flats. The results of the SMOV differential photometry characterization of NICMOS cameras indicate that relative photometry to better than 2% should be attained across the NIC1 and NIC2 detectors when on-orbit flats become available. A Cycle 7 calibration program has been designed to measure, for each camera, and with a fine grid, the photometric deviations as a function of position. A correction image might be generated as a product of this program, if measurable deviations are found.

### 3.3. Intra-pixel Sensitivity Variations

As with many other array detectors, the sensitivity of the NICMOS detectors is lower near the edge of the pixels than in their centers. It is as though there were small regions of reduced sensitivity along the intra-pixel boundaries. In practical terms this means that for

a source whose flux changes rapidly on a size comparable with or smaller than the pixel size, the measured countrate, and therefore flux, will depend on where the center of the source lies with respect to the center of the pixel. Since this is not known a priori, this effect will introduce some uncertainty in the flux calibration for a point source. This uncertainty will be largest (no more than few percent, we expect) for NIC3 at short wavelengths, for which the PSF is undersampled. For high precision photometry and to compute the amount of photometric uncertainty in a particular camera and filter combination due to this effect, subpixel dithering is recommended.

### 3.4. PSF Variations

The point spread function (PSF) of the telescope changes with time, and this can affect photometry using very small apertures (∼3–5 pixels in NIC1 & NIC2). Changes in focus are observed on an orbital timescale due mainly to thermal breathing of the telescope. In addition to this short term PSF variation there is an additional long term NICMOS component, as the cryogen evaporates and the dewar relaxes. As a result of the stress produced by the solid nitrogen on the cameras, NICMOS detectors have been moving, and are still moving, along the focus direction. The motion of the cameras is monitored twice a month and NICMOS focus updates can be periodically implemented, if required. In addition, PSF changes as a function of position in the detector. Tiny Tim simulations are recommended if high precision is required (for details see Krist 1997).

### 3.5. Aperture Corrections

The absolute photometry keywords (PHOTFNU, PHOTFLAM) provided in the header of NICMOS images are currently obtained using an aperture of 25 pixels for NIC1 and of 15 pixels for NIC2 and NIC3. It is often difficult to measure the total flux of a point source using such large apertures where the flux contribution from the extended wings of the PSF, difraction spikes, and scattered light is also included. This is in particular true in crowded fields where the extended wings of well resolved sources could overlap with each other. If no aperture correction is done, the absolute photometry will be in error, the exact amount depending on the specific aperture radius, filter and camera combination. To take into account aperture correction effects it is advisable to use Tiny Tim PSFs to measure the encircled energy curve of growth as explained in the HST Data Handbook (Voit 1997).

### 3.6. Red Leaks

Many very red targets will be observed with NICMOS at short wavelengths (i.e. $\sim 1\mu$m). For these sources the flux at $\sim 2.2$–$2.5\mu$m could be orders of magnitude larger than at $\sim 1.0\mu$m and therefore exceptionally good out-of-band blocking would be required. Pre-launch simulations indicated that for very red sources (temperature $\sim$ 700 K), the photometric errors induced by red leaks might be as large as an order of magnitude in a few filters. The filters for which red leaks might be a problem are: F090M, F095N, F097N, F108N, F110M, F110W, and F113N. Strategies involving observations in multiple filters to model the source spectral energy distribution are required in these cases. Observations of a very red star (Oph S1) have recently been obtained as part of the Cycle 7 calibration plan, the analysis is underway and the results will be posted on the NICMOS Web page.

### 3.7. Non-Zero Zeroth Read Correction

The zeroth read in a MULTIACCUM image happens 0.203 seconds after the reset of the detector. In case a bright source is being observed, this implies that a non-negligible amount of charge will be already accumulated on the detector by the time the zeroth read is performed. The consequences for the absolute calibration of bright sources (i.e. sources for which the measured countrate per pixel is in the range of about 14000 to about 25000 counts

per second) are obvious. Since the zeroth read subtraction from all subsequent reads in a MULTIACCUM exposure is the first step of the calibration processing, the handling of the detector nonlinear response by the current version of the calibration pipeline will be inaccurate. At the time of this writing (September 1997) a modification of the calibration pipeline software is under testing and MULTIACCUM images processed after the new software is installed in the pipeline should be free of the non-zero zeroth read problem. The software fix requires that the observations of bright sources be performed using the MULTIACCUM read mode where all individual readouts are returned from the spacecraft thus permitting an extrapolation of the counts back to the reset time to recover the true charge level.

### 3.8. Color Dependence of Flatfields

The strong wavelength dependence of the NICMOS flatfields limits the photometric accuracy of sources with extreme colors observed in broad-band filters. Simulations with a very red source (J–K = 5 equivalent to a 700K black-body) indicates that these photometric errors are small, around 3% or less (see Chapter 7 of NICMOS Instrument Handbook for details; MacKenty et al. 1997).

### 3.9. Velocity shifts and Photometry with Narrow-band Filters

The photometric conversion factors PHOTFLAM and PHOTFNU for all NICMOS filters are obtained from observations of continuum, emission line free, standards. The integrated flux in erg $sec^{-1}$ $cm^{-2}$ can be obtained as a function of the full width half maximum of the filter and the PHOTFLAM parameter as explained in the HST Data Handbook (Voit 1997). However, if the target has velocity shifts like the system velocity in galaxies or high velocity flows in galactic sources, and the emission line is not at the central wavelength of the filter, the line flux will be in error (in general few to several percent, depending on the filter and velocity shift) and a correction to account for the filter transmission curve is required (see details in Voit 1997).

## 4. NICMOS Absolute Photometry: Preliminary Results

### 4.1. The SMOV Absolute Photometry Tests: First On-orbit Calibration

Images of two solar analogs (P330E and P177D) and a red star (Oph S1) were taken as part of the NICMOS SMOV absolute photometry test in April (proposal ID 7049) and May (proposal ID 7152) of 1997. The two solar analogs were observed with each of the three NICMOS cameras at four (NIC1) or five (NIC2 & NIC3) different wavelengths spanning the NICMOS wavelength range. The red star Oph S1 was observed only with NIC1 and NIC2.

The NICMOS synthetic system consists of a set of response curves which give the transmission/reflectance of all the components which determine the response of the three cameras. Measurements of the detectors' DQE, filter transmissions and NICMOS mirror reflectivities were done in the laboratory. Estimates of the HST Optical Telescope Assembly (OTA) and obscuration by the secondary mirror and NICMOS cold mask have also been included. All these response curves are combined and used with the HST Synthetic Photometry package (`synphot`) to compute the predicted countrates for the observed standards, as a function of camera and filter. The predicted countrates are obtained for a specific set of gain values (5.4 e/ADU for NIC1 and NIC2 and 6.5 e/ADU for NIC3) and the results are compared with the observed countrates, that are flat-field dependent.

The results of the SMOV absolute photometry tests, i.e., the observed/predicted countrate ratios, for the three cameras are shown in Figures 1 to 3. The main results of these tests can be summarized in three major points:

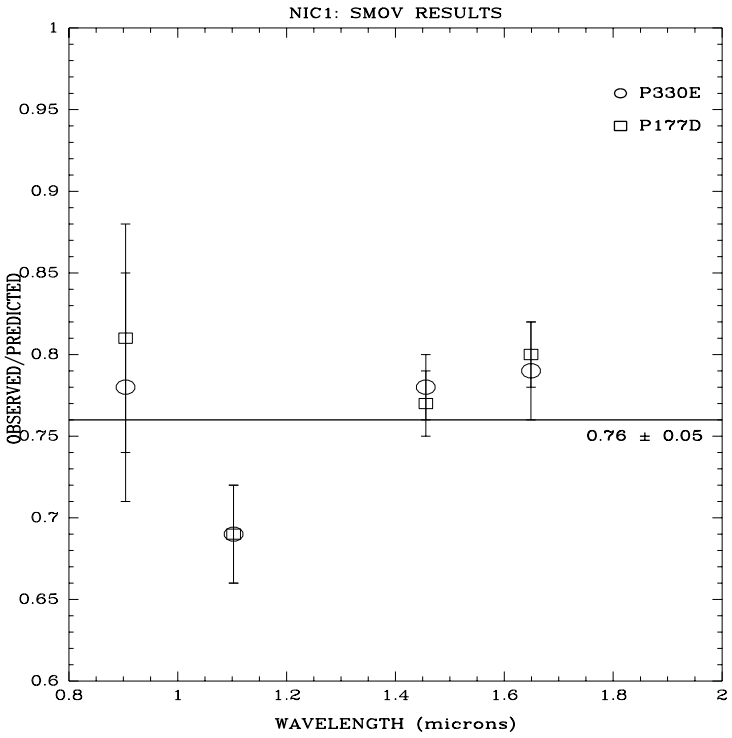


Figure 1. Results of the SMOV absolute photometry tests for NIC1

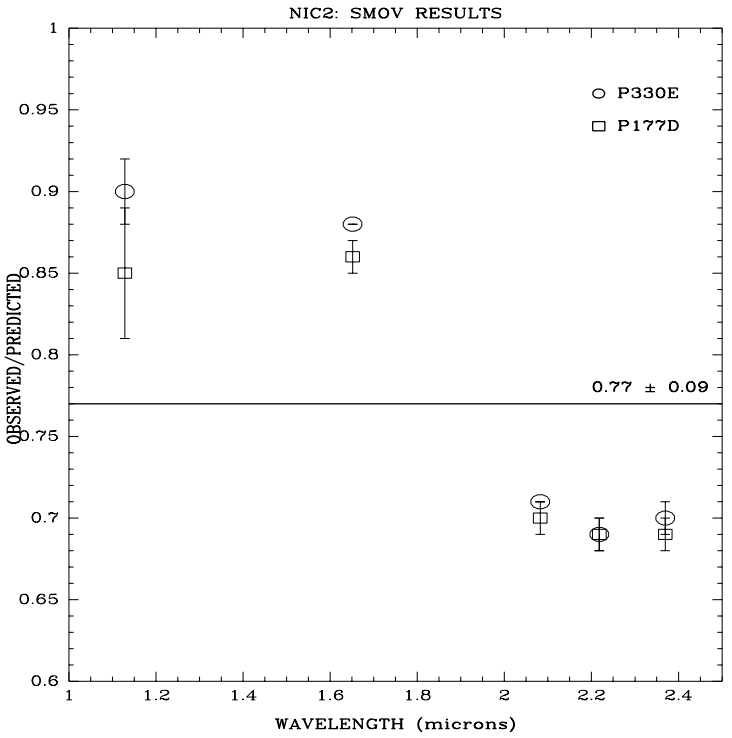


Figure 2. Results of the SMOV absolute photometry tests for NIC2

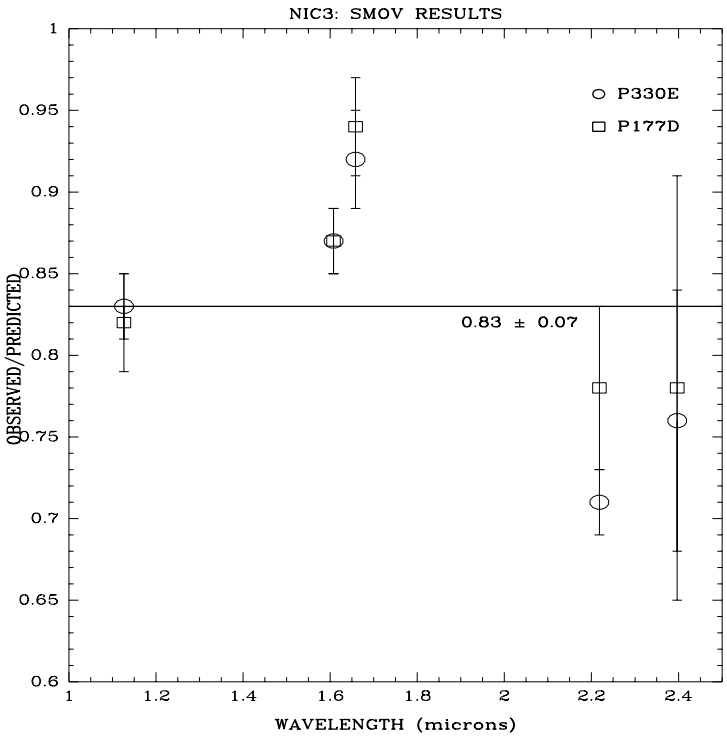


Figure 3. Results of the SMOV absolute photometry tests for NIC3

1. The observed/predicted countrates for the two standard stars agree to within the uncertainties of the measurements which were in general less than 5%. The independent measurements of the observed/predicted ratios show larger uncertainties in some filters like F090M in NIC1, and F222M and F240M in NIC3 (uncertainties at the 7% to 16% level).

2. The observed countrates are lower than the predicted values by about 10% to 30%.

3. The average ratios and uncertainties are very similar for all three cameras: $0.76 \pm 0.05$ for NIC1, $0.77 \pm 0.09$ for NIC2, and $0.83 \pm 0.07$ for NIC3.

4. There exists a smooth wavelength dependence in the ratio of observed/predicted countrates. NIC2 and NIC3 have a ratio that decreases with increasing wavelengths while the opposite seems to be true for NIC1.

In view of these results, preliminary adjustments to the prelaunch countrate predictions to match the observed countrates were implemented in July 1997. The prelaunch NICMOS throughputs were multiplied by wavelength independent factors 0.76, 0.77 and 0.83 for cameras NIC1, NIC2 and NIC3, respectively. This adjustment affected the photometric parameters delivered by the calibration pipeline and an updated photometric table (with new PHOTFLAM and PHOTFNU values) was subsequently created and delivered in July 1997. As a result of these adjustments, the current NICMOS photometric calibration (September 1997) should be correct to 10–15% for all three cameras and across the entire wavelength range covered by NICMOS, if no large normalization errors exist in the transmission curves of filters not used during SMOV.

### 4.2. Towards an Accurate Calibration: The Cycle 7 Photometric Program

High signal-to-noise images of the primary NICMOS white dwarf (G191-B2B) and solar analog (P330E) standards were taken through all the NIC1 and NIC2 narrow, medium, and broad-band filters as part of the Cycle 7 NICMOS photometric zeropoint program (proposal ID 7691). Additional images of the red star Oph S1 (J−K∼3) were obtained for a subset of filters, mostly filters at the short wavelength range, to detect any possible red leaks and quantify their contribution when very red sources are observed. No data for NIC3 were taken as part of this program (see plans for this camera in Section 6).

These data have already been calibrated with the most up-to-date version of the calibration pipeline but are still using the vacuum ground-based flats. A recalibration of the data will be done when the on-orbit flats for the different filters become available. A detailed analysis of all the data is underway but a few basic preliminary results can already be mentioned:

1. We confirm the results of the SMOV tests in the sense that there is a smooth wavelength dependence in the ratio of observed/predicted countrates with NIC1 and NIC2 going in opposite directions. This trend is observed in narrow, medium, and broad-band filters.

2. There exists an almost universal systematic difference between the observed/predicted countrate ratios obtained for the solar analog and for the white dwarf. However, the amount and trend of these differences changes from NIC1 to NIC2 and it is unlikely to be due to uncertainties in the spectral energy distribution of the standards. More analysis needs to be done before drawing any firm conclusions.

3. The observed/predicted countrate ratio for most of the filters lies within the expected 10–15% uncertainty, after the adjustment done in July 1997. However, a few filters seem to have normalization errors, the exact amount has not yet been quantified.

### 4.3. Differential Photometry Accross NICMOS Detectors

Images of a standard star (P330E) in a grid of 25 positions were taken for each of the cameras during SMOV (proposal ID 7050). The images were taken with filter F165M (NIC1 & NIC2) and F160W (NIC3). Countrates were measured for each of the 25 positions across the detectors. NIC1 and NIC3 data were calibrated with vacuum ground-based flats while NIC2 data were calibrated with both vacuum and on-orbit flats available at the time of the observations. The photometric differences normalized to the countrate measured in the central position are shown in Figures 4 and 5 for NIC1 and NIC2, respectively. The main results of these tests are:

1. NIC1 shows photometric differences at the 7% to 9% level but the photometric deviations are only 3% from the average value. It is likely that these photometric differences and deviations will be reduced when on-orbit flats become available.

2. NIC2 shows very good behaviour in terms of differential photometry. The largest photometric differences are at the ∼2% level while the deviations from the average are at the 1% level, or smaller.

3. NIC3 was heavily vignetted at the time the data were taken and the vacuum flats used in the calibration didn't give an accurate representation of the on-orbit pixel-to-pixel and large scale response of this detector.

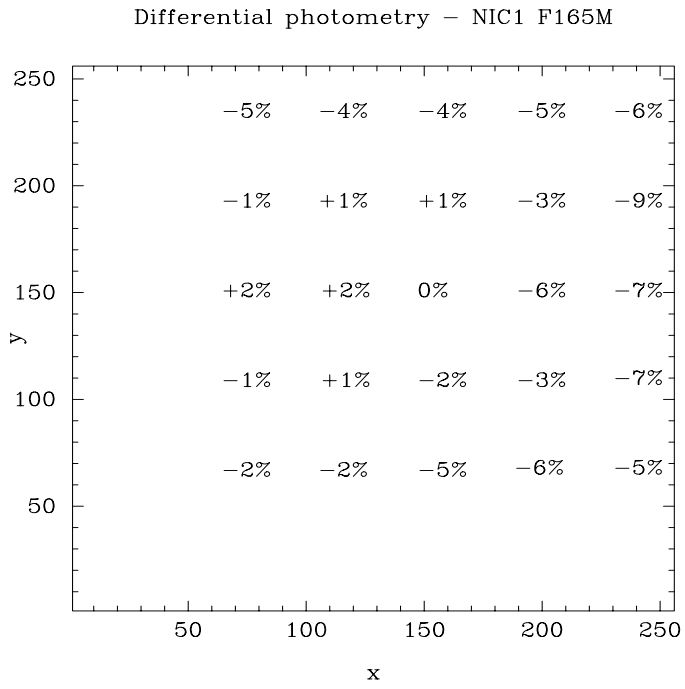


Figure 4. Results of the SMOV differential photometry test for NIC1. Values give the photometric differences with respect to the central value in percentage.

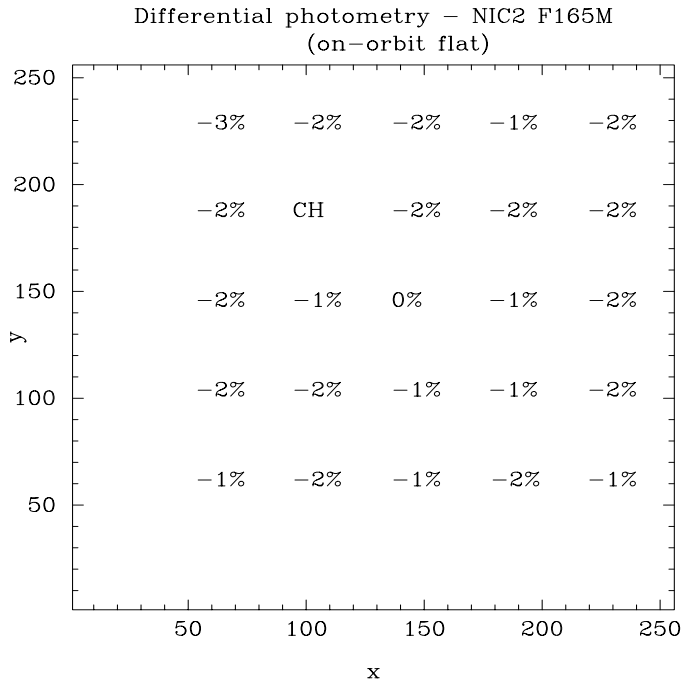


Figure 5. Results of the SMOV differential photometry test for NIC2. Values give the photometric differences with respect to the central value in percentage.

### 4.4. Photometric Stability of NICMOS Detectors

The photometric stability of NICMOS cameras is being monitored once every four weeks by taking images of one solar analog (P330E) in a subset of filters covering the NICMOS wavelength range (proposal ID 7607). These data are suplemented with additional data from SMOV proposals (7049, 7050, and 7152) to cover the first months of NICMOS after the Servicing Mission and to therefore create a longer temporal baseline.

Analysis of the data is currently underway but independent preliminary measurements by the NICMOS IDT and the NICMOS STScI groups show that the photometric stability of all three cameras during the April–August 1997 period is better than 5%, at least at 1.6$\mu$m. The photometric stability as a function of wavelength is also under investigation.

## 5. NICMOS Versus Ground-Based Magnitude Systems

The standard HST JHK system is formed by the F110W, F160W and F222M filters. NICMOS images are calibrated in units of Janskys or Janskys arcsec$^{-2}$ and currently there are no plans to compute color corrections and to provide transformations to convert HST F110W, F160W and F222M magnitudes onto ground-based magnitude systems. However, as part of the Cycle 7 absolute photometry program, a few blue stars (white dwarfs), intermediate color stars (solar analogs), and very red stars covering a large range in color ($-0.2 \leq$ J$-$K $\leq 3.0$) will be observed. Images for a white dwarf (G191B2B), a solar analog (P330E), and a red star (Oph S1) have recently been obtained. Additional standards are being considered and data for these stars could be taken in the future.

Table 1. List of Stars for Photometric Transformations

| Name | Type | H | J$-$H | H$-$K | Status |
|---|---|---|---|---|---|
| G191-B2B | white dwarf | 12.6 | $-0.10$ | $-0.14$ | data taken |
| GD71 | white dwarf | 13.8 | $-0.08$ | $-0.13$ | pending approval |
| P330E | solar analog | 11.6 | $+0.28$ | $+0.07$ | data taken |
| P177D | solar analog | 12.0 | $+0.28$ | $+0.06$ | partially taken |
| OPH-S1 | red standard | 7.3 | $+1.53$ | $+0.94$ | data taken |
| CSKE-12 | red standard | 9.5 | $+2.08$ | $+0.89$ | pending approval |
| BRI0021 | red standard | 11.1 | $+0.75$ | $+0.52$ | pendind approval |

## 6. The NIC3 Campaign and Related Calibration Plans

As a consequence of the NIC3 defocus, the Cycle 7 calibration plan has been focussed on getting an accurate calibration for NIC1 and NIC2 and on executing a limited calibration program for NIC3. In particular, the Cycle 7 absolute photometry program (proposal 7691) only obtained data to accurately calibrate NIC1 and NIC2 and no data were taken for NIC3. The photometric monitoring program (proposal ID 7607) includes observations with NIC3 in only two filters, F110W and F160W, to monitor the photometric stability of the camera and follow its behaviour. An accurate photometric calibration of the NIC3 camera will be obtained during the NIC3 campaign. This calibration includes observations at the beginning of the campaign of at least three standards (one white dwarf, one solar analog, and one red standard) using all NIC3 filters. Towards the end of the campaign, images for one standard will be taken in several filters to monitor the photometric stability of NIC3 during the campaign.

**Acknowledgments.** E. Bergeron, S. Holfeltz and C. Ritchie have contributed in several aspects to this project but in particular recalibrating SMOV and Cycle 7 data and performing most of the actual measurements reported here. Dr. E. Persson provided ground-based measurements of the solar analogs and red stars. Dr. A. Alonso analysed the data taken for the SMOV differential photometry tests. The authors thank Dr. R. Bohlin for his many contributions in defining and generating the set of NICMOS spectrophotometric standards. The authors want also to thank Dr. C. Skinner for many enlightening conversations regarding the performance and characteristics of NICMOS detectors.

## References

Bohlin, R.C., 1996, AJ, 111, 1743.

Bohlin, R.C., Colina, L., & Finley, D.S., 1995, AJ, 110, 1316.

Campins, H., Rieke, G.H., & Lebofsky, M.J., 1985, AJ, 90, 896.

Colina, L., & Bohlin, R.C., 1994, AJ, 108, 1931.

Colina, L., & Bohlin, R.C., & Castelli, F., 1996, AJ, 112, 307.

Colina, L., & Bohlin, R.C., 1997, AJ, 113, 1138.

MacKenty, J.W. et al., 1997, *NICMOS Instrument Handbook*, Version 2.0 (Baltimore: STScI).

Voit, M., 1997, *HST Data Handbook*, Version 3.0 (Baltimore: STScI).